J|A|C|S
ARTICLES
Published on Web 08/15/2006

Origin of Syn/Anti Diastereoselectivity in Aldehyde and Ketone Crotylation Reactions: A Combined Theoretical and Experimental Study

Lutz F. Tietze,*,† Tom Kinzel,† and Stefan Schmatz‡

Contribution from the Institut für Organische und Biomolekulare Chemie, Georg-August-Universität Göttingen, Tammannstrasse 2, D-37077 Göttingen, Germany, and Institut für Physikalische Chemie, Georg-August-Universität Göttingen, Tammannstrasse 6, D-37077 Göttingen, Germany

Received April 12, 2006; E-mail: ltietze@gwdg.de

Abstract: We report on experimentally determined and computationally predicted diastereoselectivities of (a) multicomponent crotylation (MCC) reactions of simple aliphatic aldehydes and ketones and (b) of acetal substitution (AS) reactions of aldehyde dimethyl acetals with *E*- and *Z*-configurated crotyl trimethylsilane to give homoallylic methyl ethers bearing two newly formed stereogenic centers. We found that corresponding MCC and AS reactions give nearly equal syn/anti ratios. While the crotylations of acetaldehyde and propionaldehyde mainly result in the syn product for *E*-configurated silane and in the anti product for *Z*-configurated silane, the syn product is found as main product for the crotylation of pivaldehyde regardless of substrate double bond geometry. Using butanone as substrate, the anti product is found as main product in both cases. By computational investigation employing the B3LYP/6-31+G(d) level of theory in dichloromethane solution (PCM/UAKS), we found that the attack of *O*-methyl-substituted carboxenium ions by crotyl silane explains the experimentally observed selectivities, indicating that these crotylations in fact proceed in an S_N1-type reaction via this ionic intermediate. Comparison of relevant open transition-state structures leads to a rationalization of the observed selectivities. For all systems studied, three transition-state conformations are necessary and sufficient to determine the selectivity. This has been confirmed by studying the MCC reactions of isobutyraldehyde. Activation energies for the stereogenic step have been determined by calculation of the transition state and substrate structures in dichloromethane solution at the B3LYP/6-311+G(2d,p)//B3LYP/6-31+G(d) level of theory in dichloromethane solution. The possibility to predict simple diastereoselectivity in general Lewis acid-mediated crotylations of aldehydes and ketones is discussed.

1. Introduction

Homoallylic alcohols and homoallylic ethers are versatile intermediates in the synthesis of many natural products and other biologically active compounds. As a consequence, numerous procedures, including enantioselective syntheses, have been developed for the synthesis of these building blocks.[1−3] Most of these procedures rely on C−C-bond formation by addition of an allylmetal to a carbonyl group which usually needs to be activated by a Lewis acid. For one-step enantioselective syntheses of homoallylic alcohols, either chiral substrates or chiral Lewis acids can be used. Prominent examples of such reactions are the employment of chiral allyl silanes,[4,5] or the enantioselective allylboration of ketones using catalytical amounts of copper fluoride and the (*R*,*R*)-^{i}Pr-DuPHOS ligand in the presence of lanthanides.[3c]

The stereoselective formation of homoallylic ethers and subsequent ether cleavage is an option in cases where the direct formation of the alcohol does not show the desired selectivity. Furthermore, this way is attractive in total syntheses in which the alcohol function is needed in the final product but must be protected in the preceding reaction steps. Homoallylic ethers can be prepared by addition of allylmetal to acetals in the presence of acids; however, to obtain stereoselectivity, at least

† Institut für Organische und Biomolekulare Chemie.
‡ Institut für Physikalische Chemie.

(1) For reviews, see: (a) Fleming, I.; Dunoguès, J.; Smithers, R. *Org. React.* **1989**, *37*, 57−575. (b) Majetich, G. In *Organic Synthesis. Theory and Applications*; Hudlicky, T., Ed.; JAI Press: Greenwich, CT, 1989. (c) Yamamoto, Y.; Asao, N. *Chem. Rev.* **1993**, *93*, 2207−2293. (d) Fleming, I.; Barbaro, A.; Walter, D. *Chem. Rev.* **1997**, *97*, 2063−2192. (e) Denmark, S. E.; Fu, J. *Chem. Rev.* **2003**, *103*, 2763−2793.
(2) Recent publications for general allylation and crotylation procedures: (a) Yasuda, M.; Hirata, K.; Nishino, M.; Yamamoto, A.; Baba, A. *J. Am. Chem. Soc.* **2002**, *124*, 13442−13447. (b) Aoyama, N.; Hamada, T.; Anabe, K.; Kobayashi, S. *Chem. Commun.* **2003**, 676−677. (c) Zha, Z.; Xie, Z.; Zhou, C.; Chang, M.; Wang, Z. *New J. Chem.* **2003**, *27*, 1297−1300. (d) Li, G.; Zhao, G. *J. Org. Chem.* **2005**, *70*, 4272−4278.
(3) Recent publications for asymmetric allylation procedures: (a) Kii, S.; Maruoka, K. *Chirality* **2003**, *15*, 68−70. (b) Cunningham, A.; Mokal-Parekh, V.; Wilson, C.; Woodward, S. *Org. Biomol. Chem.* **2004**, *2*, 741−748. (c) Wada, R.; Oisaki, K.; Kanai, M.; Shibasaki, M. *J. Am. Chem. Soc.* **2004**, *126*, 8910−8911. (d) Kim, J. G.; Waltz, K. M.; Garcia, I. F.; Kwiatkowski, D.; Walsh, P. J. *J. Am. Chem. Soc.* **2004**, *126*, 12580−12585. (e) Burgos, C. H.; Canales, E.; Matos, K.; Soderquist, J. A. *J. Am. Chem. Soc.* **2005**, *127*, 8044−8049. (f) Canales, E.; Prasad, K. G.; Soderquist, J. A. *J. Am. Chem. Soc.* **2005**, *127*, 11572−11573. (g) Wadamoto, M.; Yamamoto, H. *J. Am. Chem. Soc.* **2005**, *127*, 14556−14557.
(4) For a review, see: Masse, C. E.; Panek, J. S. *Chem. Rev.* **1995**, *95*, 1293−1316.
(5) Shing, T. K. M.; Li, L. *J. Org. Chem.* **1997**, *62*, 1230−1233.

10.1021/ja062528v CCC: $33.50

Scheme 1. Multicomponent Allylation Reaction by Markó

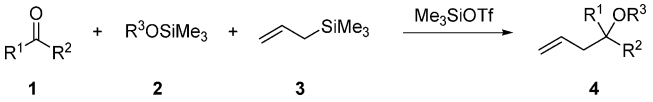

Chart 1. Examples for Chiral Silyl Ethers Used for Stereoselective Multicomponent Domino Allylation of Aldehydes and/or Ketones

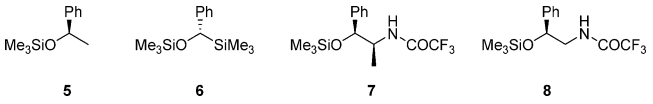

one of the substrates needs to be chiral. Markó et al. discovered a multicomponent domino[6] reaction that employed a carbonyl compound **1**, a silyl ether **2**, and allyl trimethylsilane (**3**) in the presence of trimethylsilyl trifluoromethanesulfonate (Me_3SiOTf) that yields homoallylic ethers **4** where the silyl ether moiety R^3 is transferred onto the product (Scheme 1).[7]

Several chiral auxiliaries have been developed as silyl ether components to facilitate the stereoselective formation of homoallylic ethers (Chart 1).[8−10] For practical reasons, benzyl silyl ethers such as **5**−**8** are predominantly used since the cleavage of the auxiliary residue from the resulting homoallylic ether can easily be achieved by standard methods.

When the enantiopure chiral norpseudoephedrine-derived silyl ether **7** is used, very high induced diastereoselectivities (up to >99:1) could be obtained for a number of aliphatic aldehydes and ketones.[8,11] For ketone allylation, Me_3SiOTf has to be replaced by trifluoromethanesulfonic acid (TfOH) to initiate the reaction.

Replacing unsubstituted allyl trimethylsilane by γ-substituted allyl trimethylsilanes raises the additional question of simple diastereoselectivity, as two stereogenic centers are built up in the course of the reaction. Recently, we observed that the multicomponent crotylation (MCC) reaction of butanone (**16e**), *E*- or *Z*-crotyl trimethylsilane (**9**) and the chiral auxiliary **7** in the presence of catalytic amounts of TfOH yielded mainly the anti (3*S*,4*R*)-diastereoisomer of the resulting homoallylic ether **10** with excellent induced and good to moderate simple diastereoselectivity, regardless of the starting material double bond geometry (Scheme 2).[11]

This observation is in sharp contrast to the reactions of aldehydes with crotyl silanes in the presence of Lewis acids which, together with crotyl stannanes, have been classified to give syn diastereoselectivity for the resulting homoallylic alcohol in a stereoconvergent way.[12] In these cases, it is assumed that

Scheme 2. Stereoselective MCC Reaction of Butanone (**16e**) Employing the Chiral Norpseudeoephedrine-Derived Silyl Ether **7**

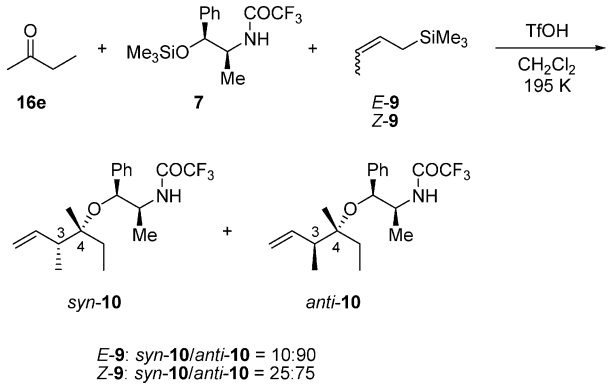

E-**9**: *syn*-**10**/*anti*-**10** = 10:90
Z-**9**: *syn*-**10**/*anti*-**10** = 25:75

Scheme 3. General Mechanism for the Formation of Homoallylic Alcohols **13** by Crotylation of Lewis-Acid Activated Aldehydes **11** with Crotyl Trimethylsilane **9**; LA = Lewis Acid, X^- = Any Nucleophile, e.g. Lewis Acid Counterion

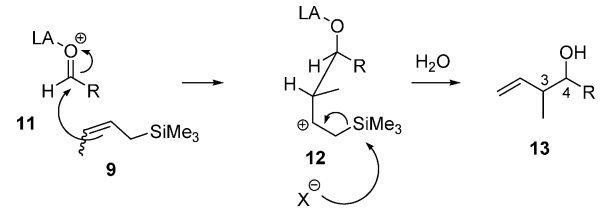

the Lewis acid coordinates to the carbonyl oxygen atom, thus forming an intermediate **11** that is much more susceptible to attack from the weak nucleophile crotyl silane than is the original aldehyde. In the following nucleophilic addition of **9** to give **12**, the stereogenic centers of the final product are generated. Subsequent nucleophilic attack at the silicon atom generates the product double bond, resulting in an overall allylic rearrangement (Scheme 3). Aqueous workup then yields the homoallylic alcohol **13**.

Assuming kinetic control, simple syn/anti diastereoselectivity of crotylation reactions solely depends on the attack of the crotyl silane to the aldehyde−Lewis acid complex. Closed, six-membered transition states (TSs) involving allyl silanes could only be found for allylating agents that are themselves Lewis acids, such as silacyclobutane derivates. Here, the formation of a dative bond generates a hypervalent silicon species that is energetically accessible because of ring strain release.[13] For allylations using allyl trialkylsilanes, a Lewis acid must be added to obtain a product. Since the oxygen atom already forms one dative bond to the added Lewis acid, closed TSs cannot be formed. In addition, closed TSs would predict an unobserved stereoconservative behavior in crotylation reactions. Hence, open TSs, where the trialkylsilicon residue is pointing away from the aldehyde−Lewis acid complex, have been proposed.[12]

The results of a number of experimental and computational investigations on allylation and crotylation reactions of Lewis-acid activated aldehydes with allyl or crotyl silanes or stannanes draw a picture of the TS structures involved. Conformational analysis of carboxenium ions and investigations on attack trajectories have been performed by Houk et al., but without

(6) (a) Tietze, L. F. *Chem. Rev.* **1996**, *96*, 115−136. (b) Tietze, L. F.; Brasche, G.; Gericke, K. *Domino Reactions in Organic Synthesis*, 1st ed.; Wiley VCH: Weinheim 2006.
(7) Mekhalfia, A.; Markó, I. E. *Tetrahedron Lett.* **1991**, *32*, 4779−4782.
(8) (a) Tietze, L. F.; Dölle, A.; Schiemann, K. *Angew. Chem., Int. Ed. Engl.* **1992**, *31*, 1372−1373. (b) Tietze, L. F.; Wegner, C.; Wulff, C. *Synlett* **1996**, 471−472. (c) Tietze, L. F.; Wegner, C.; Wulff, C. *Eur. J. Org. Chem.* **1998**, *8*, 1639−1644. (d) Tietze, L. F.; Weigand, B.; Völkel, L.; Wulff, C.; Bittner, C. *Chem. Eur. J.* **2001**, *7*, 161−168. (e) Tietze, L. F.; Hölsken, S.; Adrio, J.; Kinzel, T.; Wegner, C. *Synthesis* **2004**, *13*, 2236−2239.
(9) (a) Lindermann, R. J.; Anklekar, T. V. *J. Org. Chem.* **1992**, *57*, 5078−5080. (b) Lindermann, R. J.; Chen, K. *J. Org. Chem.* **1996**, *61*, 2441−2453. (c) Lindermann, R. J.; Chen, S. *Tetrahedron Lett.* **1995**, *43*, 7799−7802. (d) Lindermann, R. J.; Chen, S. *Tetrahedron Lett.* **1996**, *37*, 3819−3822. (e) Cossrow, J.; Rychnovsky, S. D. *Org. Lett.* **2002**, *4*, 147−150. (f) Huckins, J. R.; Rychnovsky, S. D. *J. Org. Chem.* **2003**, *68*, 10135−10145.
(10) For a general review on silicon Lewis acid mediated reactions, see: Dilman, A. D.; Ioffe, S. L. *Chem. Rev.* **2003**, *103*, 733−772.
(11) Tietze, L. F.; Völkel, L.; Wulff, C.; Weigand, B.; Bittner, C.; McGrath, P.; Johnson, K.; Schäfer, M. *Chem. Eur. J.* **2001**, *7*, 1304−1308.
(12) Denmark, S. E.; Weber, E. J. *Helv. Chim. Acta* **1983**, *159*, 1655−1660.
(13) (a) Omoto, K.; Sawada, Y.; Fujimoto, H. *J. Am. Chem. Soc.* **1996**, *118*, 1750−1755. (b) Omoto, K.; Fujimoto, H. *J. Am. Chem. Soc.* **1997**, *119*, 5366−5372. (c) Zhang, X.; Houk, K. N.; Leighton, J. L. *Angew. Chem., Int. Ed.* **2005**, *44*, 938−941.

Scheme 4. Proposed in Situ Formation of *O*-Alkylated Carboxenium Ions **15** in Multicomponent Reactions

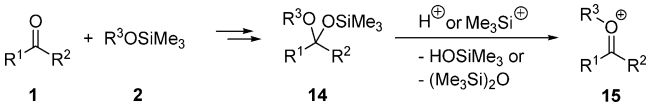

determining TS geometries.[14] Experimental evidence comes from strained, intramolecular systems,[15] whereas computational investigations have been performed only for simplified systems.[16] One TS for the attack of allyl trimethylsilane to protonated acetaldehyde has been identified.[17] Some TSs have been located for the addition of several γ-substituted allyl trimethylsilanes to a lithiated α,β-unsaturated acid, but without scanning the whole TS space.[18] Keck et al. have discussed part of the open TS space (leaving out *Z*-configurated aldehyde−Lewis acid complexes) for the crotylation of BF_3-activated aldehydes with crotyl tributylstannane on the basis of steric interaction and possible secondary overlap, but neither experimental nor computational data have been used.[19] Recently, de Lera et al. scanned the open TS space of the related Mukaiyama aldol reaction of BF_3-activated α,β-unsaturated aldehydes with 2-(trimethylsiloxy)furane.[20]

If MCC reactions are generally similar to crotylation reactions employing Lewis acids, one should expect the formation of an *O*-alkylated carboxenium ion **15** as an intermediate where the alkyl substituent acts as a positively charged Lewis acid and finally ends up as substituent at the oxygen atom of the homoallylic ether. This intermediate could be formed by acid-catalyzed dissociation of the mixed acetal **14** that is generated by formal addition of the silyl ether **2** to the carbonyl compound **1** (Scheme 4).[21]

Trehan et al. could show that the attack of allyl trimethylsilane to the mixed acetal of type **14** formed from simple aldehydes and the chiral silyl ether **5** does not proceed via an S_N2-type reaction, and thus suggested an S_N1-type reaction,[22] which is in line with the original mechanistic proposal by Markó.[7] Previous evidence for this S_N1-type mechanism comes from Sammakia et al. who proved that carboxenium ions are formed in Lewis-acid mediated reactions of acyclic dicarboacetals.[23] Polt et al. investigated the addition of allyl trimethylsilylsilane to monosilyl acetals of type **14** formed from aldehydes with regard to different Lewis acids and several residues R^3, but the results obtained did not allow for a clear mechanistic proposal.[24] Because of the nature of the chiral silyl ether **7**, an oxazolidinium intermediate that could be isolated is formed in the corresponding multicomponent allylation of aldehydes and serves as electrophile for the allylation step;[25] however, no such intermediate could be isolated when ketones were employed.

Chart 2. Carbonyl Compounds **16** and Corresponding *O*-Methyl Carboxenium Ions **17** under Investigation

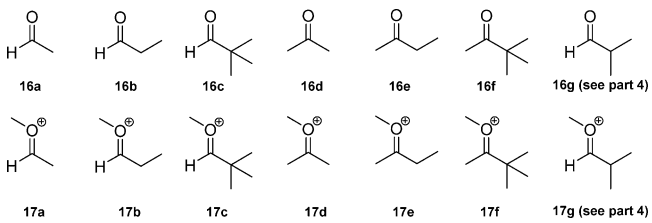

Although different mechanisms for aldehyde and ketone crotylations are suggested by the divergent stereochemical outcome of both types of reactions, it is possible that this fact could be explained by differences in the TS geometries of the stereogenic step, while maintaining the general S_N1-type mechanism displayed in Schemes 3 and 4. To find indirect evidence for the existence of the proposed carboxenium ion and to gain detailed mechanistic insight into the origin of simple syn/anti diastereoselectivities in MCC reactions of simple aliphatic aldehydes and ketones, we decided to employ a combined approach where we compare experimental selectivities with the corresponding computationally predicted quantities. Since the prediction of selectivities is based on only very small energy differences of the TSs, we were reluctant to add more uncertainty by simplifying the experimental system to fit computational needs. Consequently, we decided to use the smallest systems possible where experiments can still be performed. One set of three *O*-methyl-carboxenium ions **17a**−**c**, derived from the aliphatic aldehydes **16a**−**c**, and one set of three *O*-methyl-carboxenium ions **17d**−**f**, derived from the aliphatic methyl ketones **16d**−**f**, were chosen as electrophiles for computational investigation of the proposed stereogenic step (Chart 2). For each of these carboxenium ions, TSs for the crotylation employing *E*- and *Z*-configurated crotyl trimethylsilane were identified.

Although the crotylation of acetone (**16d**) does not yield diastereomers, it is included in this study for the sake of comparison of TS structures. For all carbonyl compounds **16a**−**f** but **16d**, experiments have been performed as MCC reactions employing trimethylsilyl methyl ether (**18**) as silyl ether component. The reaction of aldehyde or ketone dimethylacetals with crotyl silane in the presence of a Lewis or Brønsted acid (acetal substitution AS, see Scheme 5) should similarly give the corresponding *O*-methyl carboxenium ion as an intermediate.[23] To test whether MCC and AS reactions proceed with equal selectivities, AS reactions were performed with commercially available acetaldehyde and propionaldehyde dimethyl acetals **20a**−**b**. The AS reaction of pivaldehyde dimethyl acetal is well-known and is found to be syn selective with a selectivity of 97:3 (92:8) when employing *E*-(*Z*)-crotyl trimethylsilane.[26]

Following this introduction, we give details on how the computational investigation was performed. The subsequent results and dicussion section is divided into four parts: we first

(14) (a) Paddon-Row, M. N.; Rondan, N. G.; Houk, K. N. *J. Am. Chem. Soc.* **1982**, *104*, 7162−7166. (b) Broeker, J. L.; Hoffmann, R. W.; Houk, K. N. *J. Am. Chem. Soc.* **1991**, *113*, 5006−5017.
(15) (a) Denmark, S. E.; Weber, E. J. *J. Am. Chem. Soc.* **1984**, *106*, 7970−7971. (b) Denmark, S. E.; Willson, T. M. *J. Am. Chem. Soc.* **1989**, *111*, 3475−3476. (c) Denmark, S. E.; Almstead, N. G. *J. Org. Chem.* **1994**, *59*, 5130−5132. (d) Denmark, S. E.; Hosoi, H. *J. Org. Chem.* **1994**, *59*, 5133−5135.
(16) Bottoni, A.; Costa, A. L.; Di Tommaso, D.; Rossi, I.; Tagliavini, E. *J. Am. Chem. Soc.* **1997**, *119*, 12131−12135.
(17) Mayer, P. S.; Morton, T. H. *J. Am. Chem. Soc.* **2002**, *124*, 12928−12929.
(18) Organ, M. G.; Dragan, V.; Miller, M.; Froese, R. D. J.; Goddard, J. D. *J. Org. Chem.* **2000**, *65*, 3666−3678.
(19) Keck, G. E.; Savin, K. A.; Cressman, E. N. K.; Abbott, D. E. *J. Org. Chem.* **1994**, *59*, 7889−7896.
(20) López, C. S.; Álvarez, R.; Vaz, B.; Faza, O. N.; de Lera, Á. R. *J. Org. Chem.* **2005**, *70*, 3654−3659.
(21) (a) Tsunoda, T.; Suzuki, M.; Noyori, R. *Tetrahedron Lett.* **1980**, *21*, 1357−1358. (b) Noyori, R.; Murata, S.; Suzuki, M. *Tetrahedron* **1981**, *37*, 3899−3910.
(22) Manju, K.; Trehan, S.; *Chem. Commun.* **1999**, 1929−1930.
(23) Sammakia, T.; Smith, R. S. *J. Am. Chem. Soc.* **1994**, *116*, 7915−7916.
(24) Sames, D.; Liu, Y.; DeYoung, L.; Polt, R. *J. Org. Chem.* **1995**, *60*, 2153−2159.
(25) Tietze, L. F.; Wulff, C.; Wegner, C.; Schuffenhauer, A.; Schiemann, K. *J. Am. Chem. Soc.* **1998**, *120*, 4276−4280.
(26) Hosomi, A.; Ando, M. Sakurai, H. *Chem. Lett.* **1986**, 365−368.

Scheme 5. Crotylation Reactions Performed in the Present Study

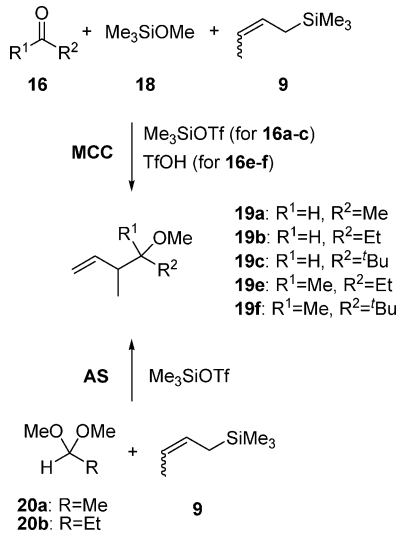

present the performed experiments before we describe how selectivities were predicted computationally. Then, we discuss TS energies and geometries and conclude with a subsection on activation energies for the stereogenic step. To examine the predictive capability of our results up to that point, we studied the MCC reaction of isobutyraldehyde **16g**. The paper ends with conclusions that we can draw from this investigation. Experimental procedures and other information can be found in the Supporting Information.

2. Computational Methods and Strategy

The syn/anti diastereoselectivity for the addition of *E*- and *Z*-crotyl trimethylsilane to *O*-methylated carboxenium ions has been determined computationally by employing reaction rate coefficients calculated according to transition state theory. Since there are more TSs than only a single one possible for the formation of each diastereomer, eq 1 has been used to obtain the syn product ratios PR_{syn}, where $G_{rel,i}^{\ddagger}$ denotes the free energy difference between the *i*th transition state and the transition state with lowest free energy.

$$PR_{syn} = \sum_{i \in TS_{syn}} \exp\left(-\frac{G_{rel,i}^{\ddagger}(T)}{RT}\right) \Bigg/ \sum_{j \in TS_{syn,anti}} \exp\left(-\frac{G_{rel,j}^{\ddagger}(T)}{RT}\right) \times 100\% \quad (1)$$

To minimize the computational effort, the following strategy has been employed: First, we identified all TSs for a model system bearing an SiH_3 group instead of the $SiMe_3$ residue at the crotyl silane (in the following, called "simplified system"). From this set of TSs, only those with a free energy difference of $G_{rel}^{\ddagger} \leq 9$ kJ mol^{-1} to the energetically lowest TS (in the following, termed "relevant TSs") were selected for further investigation. According to eq 1, any energetically higher TS contributes less than 3% to the product ratio at $T = 195$ K in the limiting case of only one relevant TS. However, in all actual cases of the present work, two or more relevant TSs could be identified. Consequently, higher-energy TSs can be neglected without any loss of accuracy.

After replacement of the SiH_3 group of the relevant TSs by the actual $SiMe_3$ group (in the following, called "actual system"), full geometry optimizations and subsequent frequency analyses were carried out. Therefrom, we obtained — within the harmonic oscillator−rigid rotor approach — the free energy values needed to determine the selectivity of the actual system according to eq 1.

In this work, only the energies of saddle point structures are of primary importance for the evaluation of the diastereomeric ratio, while absolute reaction barrier heights play only a minor role. Thus, is was necessary to choose a density functional that is particularly well suited for the calculation of transition states.

Most existing exchange-correlation functionals are hybrid functionals which mix small fractions (15−25%) of exact (Hartree−Fock or Kohn−Sham) exchange with the "generalized gradient" approximation (GGA) exchange.[27a] It is well-known that these functionals show deficiencies with respect to their performance in calculating barrier heights[28] which are often underestimated, and sometimes even no barrier is found on the potential energy surface. As was shown by Durant[28b] 10 years ago, a hybrid functional with 50% exact exchange, the BH&HLYP (Becke half-and-half and LYP correlation) functional,[29] yields reasonable barrier heights, while the popular B3LYP functional[27] (only 20% exact exchange) resulted in much better data for ground state and, in particular, thermochemical properties. Other functionals have been designed particularly for the calculation of saddle point structures, based on existing functionals. Lynch et al.[30] reparametrized the modified Perdew−Wang functional[31] and proposed the MPW1K (modified Perdew−Wang for kinetics) with 43% exact exchange, while Kang and Musgrave[32] started from B3LYP and included 56% exact exchange (KMLYP). However, the gain in accuracy of the calculated barrier heights is counterbalanced by the larger errors in several ground-state properties such as geometries and atomization energies with deviations 2−3 times larger than those obtained with conventional hybrid functionals.[33] Recently, Becke has proposed a new exact-exchange-based functional for dynamical and nondynamical correlation[34] which when tested for 70 reactions (hydrogen and heavy atom transfer, nucleophilic substitutions, association and unimolecular reactions; including both even- and odd-electron systems) yielded a mean absolute error of 1.4 kcal mol^{-1} with respect to accurate reference data.[35]

All calculations in this work were carried out using the Gaussian 03[36] program package. All geometry optimizations and frequency calculations for the simplified system were performed at the BH&HLYP/6-31+G(d,p) level of theory for isolated (gas-phase) systems and $T = 298$ K. To verify the nature of the identified first-order saddle points, the normal mode with imaginary frequency was analyzed. For some TSs, additional IRC calculations[37] have been performed. The selection of relevant TSs was based on their relative free energy $G_{rel}^{\ddagger}$ at 298 K. In addition, $G_{rel}^{\ddagger}$ has been determined for $T = 195$ K and 273 K to predict selectivities for the simplified system in the gas phase.

After selection, TS free energies for the actual system in dichloromethane solution were obtained using the B3LYP/6-31+G(d) level of theory in combination with the polarized continuum model (PCM) as described by Tomasi et al. and Barone et al.,[38,39] with UAKS radii for both temperatures 195 and 273 K. It should be noted that the UAKS and UAHF sets of radii are identical for the investigated systems. Both optimizations and frequency analyses were performed for the conditions in solution. Again, the nature of the stationary points found was verified

(27) (a) Becke, A. D. *Phys. Rev. A* **1988**, *38*, 3098−3100. (b) Lee, C.; Yang, W.; Parr, R. G. *Phys. Rev. B* **1988**, *37*, 785−789. (c) Becke, A. D. *J. Chem. Phys.* **1993**, *98*, 5648−5652.
(28) (a) Baker, J.; Andzelm, J.; Muir, M.; Taylor, P. R. *Chem. Phys. Lett.* **1995**, *237*, 53−60. (b) Durant, J. L. *Chem. Phys. Lett.* **1996**, *256*, 595−602.
(29) Becke, A. D. *J. Chem. Phys.* **1993**, *98*, 1372−1377.
(30) (a) Lynch, B. J.; Fast, P. L.; Harris, M.; Truhlar, D. G. *J. Phys. Chem. A* **2000**, *104*, 4811−4815. (b) Lynch, B. J.; Truhlar, D. G. *J. Phys. Chem. A* **2001**, *105*, 2936−2941.
(31) Adamo, C.; Barone, V. *J. Chem. Phys.* **1998**, *108*, 664−675.
(32) Kang, J. K.; Musgrave C. B. *J. Chem. Phys.* **2001**, *115*, 11040−11051.
(33) Boese, A. D.; Martin, J. M. L.; Handy, N. C. *J. Chem. Phys.* **2003**, *119*, 3005−3014.
(34) Becke, A. D. *J. Chem. Phys.* **2005**, *122*, 064101.
(35) Dickson, R. M.; Becke, A. D. *J. Chem. Phys.* **2005**, *123*, 111101.
(36) Frisch, M. J.; et al. *Gaussian 03*, Revision B.04; Gaussian, Inc.: Wallingford, CT, 2004.
(37) (a) Gonzalez, C.; Schlegel, H. B. *J. Chem. Phys.* **1989**, *90*, 2154−2161. (b) Gonzalez, C.; Schlegel, H. B. *J. Phys. Chem.* **1990**, *94*, 5523−5527. (c) Gonzalez, C.; Schlegel, H. B. *J. Chem. Phys.* **1991**, *95*, 5853−5860.
(38) (a) Mennuci, B.; Cammi, R.; Tomasi, J. *J. Chem. Phys.* **1999**, *110*, 6858−6870. (b) Cossi, M.; Scalmani, G.; Rega, N.; Barone, V. *J. Chem. Phys.* **2002**, *117*, 43−54.
(39) For a review on continuum solvation models, see: Tomasi, J.; Mennucci, B.; Cammi, R. *Chem. Rev.* **2005**, *105*, 2999−3093.

Table 1. Reaction Details and Experimental Results of Crotylation Reactions with Crotyl Trimethylsilanes[a]

entry	reaction	product	type	*T* [K]	syn:anti	entry	reaction	product	type	*T* [K]	syn:anti
1	**16a** + *E*-**9**	**19a**	MCC	195	82:18	17	**16c** + *E*-**9**	**19c**	MCC	195	98:2
2	**20a** + *E*-**9**	**19a**	AS	195	80:20	18	**16c** + *E*-**9**	**19c**	MCC	273	98:2
3	**16a** + *E*-**9**	**19a**	MCC	273	72:28	19	**16c** + *Z*-**9**	**19c**	MCC	195	95:5
4	**20a** + *E*-**9**	**19a**	AS	273	70:30	20	**16c** + *Z*-**9**	**19c**	MCC	273	92:8
5	**16a** + *Z*-**9**	**19a**	MCC	195	31:69						
6	**20a** + *Z*-**9**	**19a**	AS	195	29:71	21	**16e** + *E*-**9**	**19e**	MCC	195	26:74
7	**16a** + *Z*-**9**	**19a**	MCC	273	34:66	22	**16e** + *E*-**9**	**19e**	MCC	273	39:61
8	**20a** + *Z*-**9**	**19a**	AS	273	30:70	23	**16e** + *Z*-**9**	**19e**	MCC	195	27:73
						24	**16e** + *Z*-**9**	**19e**	MCC	273	38:62
9	**16b** + *E*-**9**	**19b**	MCC	195	89:11						
10	**20b** + *E*-**9**	**19b**	AS	195	87:13	25	**16f** + *E*-**9**	**19f**	MCC	195	n.d.
11	**16b** + *E*-**9**	**19b**	MCC	273	81:19	26	**16f** + *E*-**9**	**19f**	MCC	273	n.d.
12	**20b** + *E*-**9**	**19b**	AS	273	80:20	27	**16f** + *Z*-**9**	**19f**	MCC	195	n.d.
13	**16b** + *Z*-**9**	**19b**	MCC	195	45:55	28	**16f** + *Z*-**9**	**19f**	MCC	273	n.d.
14	**20b** + *Z*-**9**	**19b**	AS	195	43:57						
15	**16b** + *Z*-**9**	**19b**	MCC	273	48:52						
16	**20b** + *Z*-**9**	**19b**	AS	273	45:55						

[a] MCC = Multicomponent Crotylation, AS = Dimethylacetal Substitution, n.d. = not determined.

by inspection of the normal modes with imaginary frequency. For all calculations in solution reported in this work, tight SCF convergence criteria (via keyword *SCF=Tight*) were applied. For the systems **17c** + *E*-**9**, **17d** + *E*-**9**, **17e** + *E*-**9**, and **17e** + *Z*-**9**, optimizations and frequency calculations for the actual system had to be performed employing a larger [using keyword *Integral(Grid=UltraFine)*] than the standard grid [*Integral(Grid=FineGrid)*] for both optimization and frequency analysis to find the right TSs.[40]

For the system **17a** + *E*-**9**, one of the relevant TSs (**a2-e**) (for nomenclature see later) could not be found for the actual system. Here, relevant TSs of the simplified system were re-optimized at BH&HLYP/6-31+G(d,p) level of theory in dichloromethane solution using the PCM/UAKS model.

Geometry optimizations and frequency analyses of the substrate *E*- or *Z*-crotyl trimethylsilane and the carboxenium ion were carried out at the level of theory the same as that for the corresponding TSs. For the determination of activation energies $\Delta G^{\ddagger}$, *single-point* B3LYP/6-311+G(2d,p) calculations in combination with the PCM/UAKS model at 195 and 273 K have been performed. The free energies of both substrates and TSs were obtained by adding the free energy correction term (obtained at the lower level of theory) to the *single-point* energy that comprises the potential energy and the solvation free energy contribution. The larger basis set was chosen to minimize the basis set superposition error (BSSE). In this work, we employ the difference between the free energies of the lowest-lying TS and the sum of the corresponding values of the two substrates as a measure for the activation energy $\Delta G^{\ddagger}$ for the underlying elementary step. We found that relative TS energies $G_{rel}^{\ddagger}$ differ only very slightly when applying this two-step procedure, meaning that the BSSE in these cases is a systematic error that vanishes when determining the relative energies.

3. Results and Discussion

3.1. Experiments. Scheme 5 displays the experiments that have been performed to determine the diastereoselectivities in crotylation reactions of aldehydes **16a**−**c**, aldehyde dimethylacetals **20a**−**b** as well as ketones **16e**−**f** in dichloromethane as solvent for $T = 195$ K and 273 K. The two crotylation agents *E*- and *Z*-crotyl trimethylsilane (*E*-**9** and *Z*-**9**) have been synthesized according to methods reported in the literature[11,41] in excellent diastereoselectivities (≥99:1, determined by GC analysis). For MCC reactions, trimethylsilyl methyl ether (**18**) was added as silyl ether component.

MCC reactions with aldehydes were performed according to Markó's protocol as modified by Rychnovsky et al.,[7,9f] but with dichloromethane as solvent. In the presence of 20 mol % Me_3SiOTf, 1 equivalent of silyl ether was reacted with 1.1 equivalents of both aldehyde and crotyl trimethylsilane. MCC reactions with ketones were carried out according to our procedure by reaction of 1 equivalent of silyl ether, 2 equivalents of ketone, and 2 equivalents of crotyl trimethylsilane in the presence of 20 mol % TfOH.[11] For AS reactions, 1 equivalent of dimethylacetal was reacted with 1 equivalent crotyl trimethylsilane in the presence of 1 mol % Me_3SiOTf. This catalytic amount of Lewis acid was used in the reaction of pivaldehyde dimethylacetal with crotyl trimethylsilane as published by Sakurai et al.[26] In accordance with our previous experiments, the reaction times are in the order of 3−5 days.[11] An optimization of the reaction conditions with respect to the reaction time, concentration of the substrates or the catalyst loading has not been attempted. However, we investigated the influence of the reaction time on the stereoselectivity for the AS reaction of **20a** and *Z*-**9** at $T = 273$ K. Employing a reaction time of 5 h and 3 d, respectively, no change of selectivity was observed. We therefore conclude that the selectivity is not at all time-dependent.

The diastereoselectivities of the products were determined by GC analysis on an achiral phase of the crude product obtained after aqueous workup. The crude product was purified once by column chromatography to identify the associated GC signals. GC-determined selectivities are found to be identical to those determined from analysis of ^{1}H NMR and ^{13}C NMR spectra. Table 1 quotes the experimental results.

While sensitive GC−MS experiments did not detect any observable amounts of the expected homoallylic ether **19f** in the crude mixtures obtained from crotylation reactions of **16f**, ^{1}H NMR spectra give indication that traces of the product might be present. However, these amounts did not allow for the determination of the selectivity of the reaction. The extremely low yield can be rationalized by the rather high activation energy of the stereogenic step that is calculated to be higher than 115 kJ mol^{-1} (see Table 5).

(40) On grid size effects in DFT calculations, see: (a) Martin, J. M. L.; Bauschlicher, C. W., Jr.; Ricca, A. *Comput. Phys. Commun.* **2001**, *133*, 189−201. (b) Malagoli, M.; Baker, J. *J. Chem. Phys.* **2003**, *119*, 12763−12768.

(41) Kamachi, T.; Kuno, A.; Matsuno, C.; Okamoto, S. *Tetrahedron Lett.* **2004**, *45*, 4677−4679.

Table 2. ^{1}H NMR Coupling Constants of the Homoallylic Ether Double Bond for the Assignment of Stereochemistry

		syn			anti		
entry	product	$^3J_{cis}$ [Hz]	$^3J_{trans}$ [Hz]	Δ^3J [Hz]	$^3J_{cis}$ [Hz]	$^3J_{trans}$ [Hz]	Δ^3J [Hz]
1	**19a**	10.0	17.6	7.6	10.9	16.8	5.9
2	**19b**	10.6	18.2	7.6	11.2	16.5	5.3
3	**19c**	10.2	17.2	7.0	10.7	17.0	6.3
4	**19e**	10.3	17.2	6.9	10.8	17.0	6.2

We found that the MCC and AS reactions of **16a**−**b** and **20a**−**b**, respectively, resulted in almost identical selectivities for the respective systems. In addition, the selectivities for MCC reactions **16c** + *E*-**9** and **16c** + *Z*-**9** are consistent with the results of the corresponding known AS reactions.[26] This result strongly indicates that these reactions proceed via the same intermediate, with the proposed carboxenium ion being a reasonable candidate.

Three different stereochemical outcomes are observed: The reactions of **16a** and **16b** yield the syn products *syn*-**19a** and *syn*-**19b**, respectively, when *E*-**9** is employed, while the anti products *anti*-**19a** and *anti*-**19b** are found when the *Z*-**9** is used (in the following termed "stereoconservative behavior"). For the crotylation of **16c**, the syn product *syn*-**19c** is observed regardless of the crotyl trimethylsilane double bond geometry (in the following termed "synconvergent behavior"). In accordance with our previous MCC experiment of **16e** with the chiral silyl ether **7**,[11] the anti product *anti*-**19e** is formed in the MCC reaction of **16e** and **18** with both *E*-**9** and *Z*-**9** (in the following termed "anticonvergent behavior").

Assignment of the Stereoisomers. From the found equivalence of MCC and AS reactions, we conclude that the main product found for the MCC reaction of **16c** + *E*-**9** and **16c** + *Z*-**9** corresponds to the main product found in the respective AS reaction. Sakurai et al. reported the main product to be the syn isomer of **19c**.[26] For the assignment of the stereoisomers found for the other reactions, we compared the ^{1}H NMR spectra and found that there is a pattern regarding the $^3J_{cis}$ and $^3J_{trans}$ coupling constants for the hydrogen atoms at the homoallylic ether double bond (Table 2). We found that for one of the isomers, the cis coupling constant is always larger than that for the other isomer, while the trans coupling constant is lower. Therefore, the difference of these coupling constants can be taken as a measure to distinguish and assign the isomers. Since we know the main product for the reactions of **16c** + *E*-**9** and **16c** + *Z*-**9** to be *syn*-**19c**, we can use this as a standard for the correlation.

In addition, we found that the chemical shift for 2-H is larger for the anti compound for all examples investigated (^{1}H NMR in C_6D_6, see Supporting Information). While this difference is small in the case of **19a** and **19b** (0.003 and 0.06 ppm, repectively), it is rather large for **19c** and **19e** (0.31 and 0.26 ppm, respectively). In any case, these data can be used to assign the syn- and the anti products.

3.2. Calculation of Stereoselectivities. We consider the attack of an *O*-methylated carboxenium ion by *E*- or *Z*-crotyl trimethylsilane to be the stereogenic center-forming step of both MCC and AS reactions given in Scheme 5. Assuming kinetic control, we have investigated the TSs for this step to predict the syn/anti diastereoselectivities.

Chart 3. Open Transition States for the Attack of *E*-Crotyl Trimethylsilane to *O*-Methyl-Substituted Carboxenium Ions. R^1 = H, Me; R^2 = Me, Et, ^{t}Bu; R^3 = CH_2SiH_3 (Simplified System), CH_2SiMe_3 (Actual System)

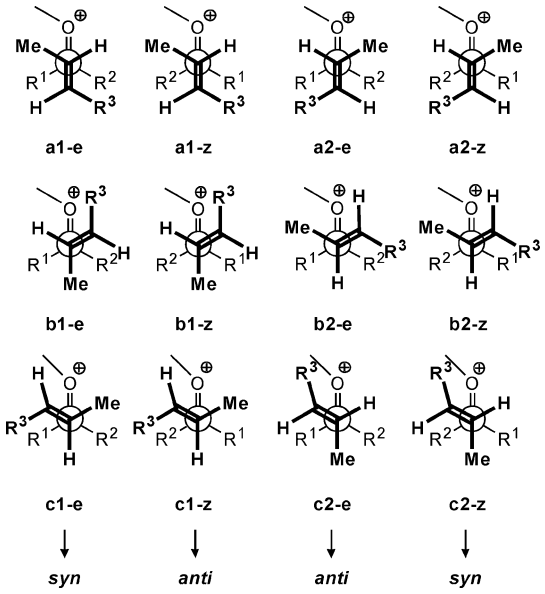

Chart 4. Open Transition States for the Attack of *Z*-Crotyl Trimethylsilane to *O*-Methyl-Substituted Carboxenium Ions; R^1 = H, Me; R^2 = Me, Et, ^{t}Bu; R^3 = CH_2SiH_3 (Simplified System), CH_2SiMe_3 (Actual System)

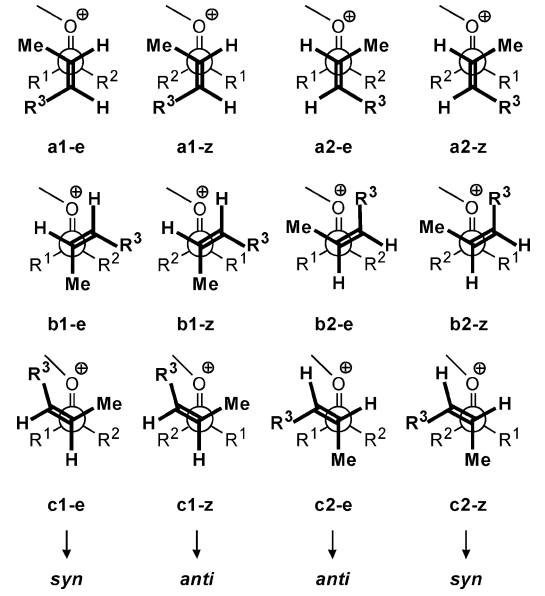

Conformations of open TSs used as starting points for geometry optimizations are shown in Charts 3 and 4 for the attack of *E*-**9** and *Z*-**9**, respectively. Each TS conformation corresponds to one product diastereomer shown below. There are three conformations distinguished by the relative orientation of the carboxenium ion and crotyl silane double bonds represented by small letters **a**, **b**, and **c**. Structures where the *si* and *re* faces of the silane attacks are depicted by **1** and **2**, respectively. Overall, 12 open TSs are possible because prochiral carboxenium ions can exist in the *E*- or *Z*-configuration, represented by **e** and **z**. For each TS, there is an enantiomeric structure possible when the silane attacks from the backside of

Table 3. Predicted and Experimentally Determined Syn/Anti Diastereoselectivities for Crotylation Reactions[e]

entry	elementary reaction	$T = 195$ K				$T = 273$ K			
		a	*b*	*c*	*d* (exptl)	*a*	*b*	*c*	*d* (exptl)
1	**17a** + *E*-**9**	**92**:8	**89**:11	n.c.	**81**:19	**87**:13	**84**:16	n.c.	**71**:29
2	**17a** + *Z*-**9**	**87**:13	**69**:31	25:**75**	30:**70**	**77**:23	**63**:37	28:**72**	32:**68**
3	**17b** + *E*-**9**	**95**:5	**89**:11	**70**:30	**88** :12	**90**:10	**84**:16	**72**:28	**81**:19
4	**17b** + *Z*-**9**	**95**:5	**75**:25	40:**60**	44:**56**	**87**:13	**69**:31	45:**55**	47:**53**
5	**17c** + *E*-**9**	**99**:1	n.c.	**98**:2	**98**:2	**98**:2	n.c.	**96**:4	**98**:2
6	**17c** + *Z*-**9**	**74**:26	**91**:8	**99**:1	**95**:5	**68**:32	**86**:14	**98**:2	**92**:8
7	**17e** + *E*-**9**	38:**62**	22:**78**	19:**81**	26:**74**	43:**57**	34:**66**	28:**72**	39:**61**
8	**17e** + *Z*-**9**	22:**78**	27:**73**	39:**61**	27:**73**	32:**68**	30:**70**	**53**:47	38:**62**
9	**17f** + *E*-**9**	**77**:23	38:**62**	18:**82**	n.d.	**70**:30	42:**58**	22:**78**	n.d.
10	**17f** + *Z*-**9**	**63**:37	17:**83**	39:**61**	n.d.	**59**:41	24:**76**	47:**53**	n.d.

[a] Simplified system ($SiMe_3 \rightarrow SiH_3$) in gas phase, BH&HLYP/6-31+G(d,p). [b] Simplified system ($SiMe_3 \rightarrow SiH_3$) in dichloromethane solution, BH&HLYP/6-31+G(d,p). [c] Actual system in dichloromethane solution, B3LYP/6-31+G(d). [d] Experimental results: for entries 1−4, averaged experimental results from MCC and AS reactions; for entries 5−10, results from MCC reactions. n.c. = not calculated because one or more relevant transition states could not be located. n.d. = not determined because of low yield. [e] For better readability, the ratio of the main product is shown in bold numbers

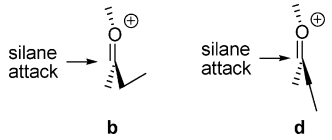

Figure 1. Additional conformational degree of freedom for transition states involving **17b** and **17e**.

the carboxenium ion. However, since enantiomeric TSs have exactly the same energy as their respective counterparts, we do not consider them in the present study. Comprehensive charts of open TSs for related reactions have been published elsewhere.[1a,d,e,4,19]

For carboxenium ions **17b** and **17e** where R^2 = Et, the number of possible TSs increases to a total number of 24, as the ethyl group can point either "backwards" or "downwards" (Figure 1), depicted by the additional descriptor **b** or **d**, respectively.

When we started our investigations of the TSs involved, we used simplified systems where the $SiMe_3$ residue was replaced by a SiH_3 group ($R^3 = CH_2SiH_3$). We planned on identifying a method for one system that reproduces the experimental data well, and then apply this method for all systems studied.

Since the prediction of selectivity relies on very small TS energy differences that are within the commonly accepted accuracy of any density functional theory (DFT) method, it was crucial that the same method was used for *all* systems to obtain comparable results. We were eager to employ the MPW1K functional, which is a modified MPW1PW91 functional especially designed to obtain very precise TS energies, that are needed to accurately calculate the selectivity.[30] At the same time, we were testing the B3LYP functional that has been established as a standard method for the calculation of ground-state molecular geometries because of its robustness and good experiment-reproducing capabilities. The basis set 6-31+G(d,p) has been employed in both cases. The diffuse basis functions allow for an adequate description of the loose bonding situation in the TSs.[42]

An identification of all TSs using MPW1K was possible for the ketone-derived systems, but not for the aldehyde-derived systems. A similar result was obtained with B3LYP; however, while in this case all TSs for the aldehyde-derived systems could be found, this was not possible for the ketone-derived systems.

(42) Lynch, B. J.; Zhao, Y.; Truhlar, D. G. *J. Phys. Chem. A* **2003**, *107*, 1384−1388.

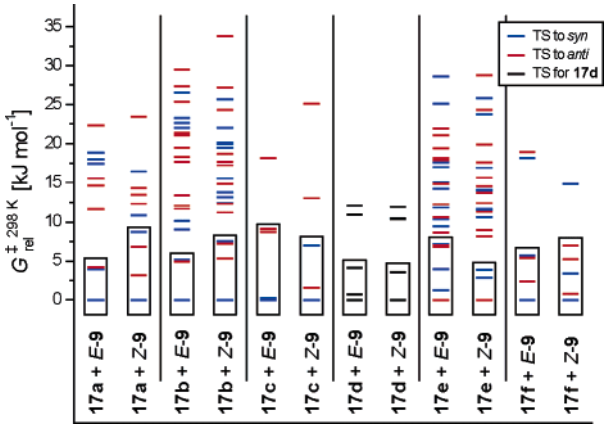

Figure 2. Relative transition-state free energies $G_{rel}^{\ddagger}$ for all simplified systems ($SiMe_3 \rightarrow SiH_3$) obtained at the BH&HLYP/6-31+G(d,p) level of theory for $T = 298$ K. All transition states contained in the rectangles were selected for further investigation.

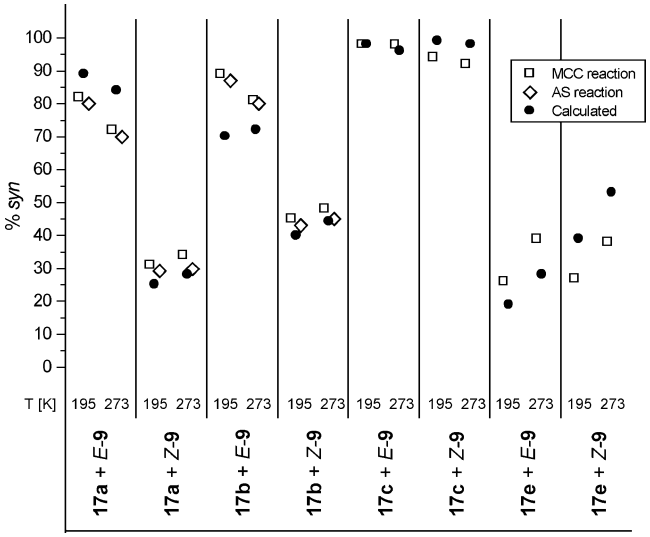

Figure 3. Comparison of experimentally determined and predicited selectivities. All predictions with B3LYP/6-31+G(d) in dichloromethane solution for the actual system except **17a** + *E*-**9** [BH&HLYP/6-31+G(d,p) in dichloromethane solution for the simplified system ($SiMe_3 \rightarrow SiH_3$)].

In each case, the TSs not found by one method were those that the other method described as low-energy TSs; therefore, neglecting them was not possible. In the course of trying to find these TSs, we set up relaxed potential energy surface (RPES) scan calculations by successively decreasing the distance

Table 4. Free Energies (Relative to the Lowest-Lying Transition State) and Selected Geometrical Parameters (see Figure 5) for Relevant Transition States Obtained at the B3LYP/6-31+G(d) Level of Theory in the Solvent Dichloromethane for the Actual Systems except for **17a** + *E*-**9** where the Transition States Obtained at BH&HLYP/6-31+G(d,p) Level of Theory in Solution for the Simplified System Are Described[a]

system	TS conformation	product stereochemistry	$G_{rel}^{\ddagger}$, 195 K [kJ mol^{-1}]	$G_{rel}^{\ddagger}$, 273 K [kJ mol^{-1}]	*d* [Å]	α [deg]	γ [deg]
17a + *E*-**9**	**b1-e**	*syn*	0	0	2.068	110.1	−73.9
	ac1-e	*syn*	2.31	2.05	2.018	105.9	104.8
	a2-e	*anti*	2.95	2.94	2.065	100.5	−177.2
17a + *Z*-**9**	**a2-e**	*anti*	0	0	2.285	98.5	177.3
	b1-e	*syn*	1.80	2.26	2.266	109.4	−70.9
	ac1-e	*syn*	7.33	7.80	2.142	102.8	133.2
	b2-e	*anti*	8.37	9.19	2.156	113.2	−61.4
17b + *E*-**9**	**b1-e-b**	*syn*	0	0.02	2.322	108.4	−73.8
	ac1-e-b	*syn*	0.42	0	2.191	104.6	107.5
	a2-e-b	*anti*	0.48	0.62	2.279	98.9	−177.4
17b + *Z*-**9**	**a2-e-b**	*anti*	0	0	2.255	98.8	177.4
	b1-e-b	*syn*	0.85	0.99	2.254	109.3	−71.0
	ac1-e-b	*syn*	3.38	2.93	2.145	102.7	132.3
	b2-e-b	*anti*	4.65	4.62	2.152	113.0	−62.1
17c + *E*-**9**	**ac1-e**	*syn*	0	0	2.172	102.5	106.9
	b1-e	*syn*	4.21	4.97	2.136	105.6	−75.6
	a2-e	*anti*	5.94	6.85	2.145	98.7	−177.2
17c + *Z*-**9**	**ac1-e**	*syn*	0	0	2.132	102.0	125.5
	b1-e	*syn*	7.95	8.36	2.132	105.7	−75.1
	b2-e	*anti*	8.04	9.12	2.086	110.2	−63.6
17d + *E*-**9**	**a2**		0	0	2.079	99.5	−174.5
	c1		4.94	6.97	2.052	104.3	90.4
	b1		5.55	6.03	2.090	104.6	−69.3
17d + *Z*-**9**	**a2**		0	0	2.066	99.6	−178.0
	b1		2.50	0.24	2.082	105.2	−65.3
	c1		10.31	10.31	2.069	106.5	72.9
17e + *E*-**9**	**a2-e-b**	*anti*	0	0	2.048	99.8	−174.7
	a2-z-b	*syn*	2.87	2.87	2.063	99.9	−171.6
	b1-e-b	*syn*	4.94	6.16	2.062	104.8	−67.9
	c1-e-b	*syn*	6.39	6.39	2.027	104.1	92.6
	b1-z-b	*anti*	9.44	9.13	2.065	104.5	−70.3
	a2-e-d	*anti*	10.22	10.66	2.041	99.1	−178.4
17e + *Z*-**9**	**a2-e-b**	*anti*	0	0.21	2.027	100.1	−179.0
	a2-z-b	*syn*	0.76	0	2.050	100.0	−173.7
	b1-e-b	*syn*	7.57	8.22	2.061	105.1	−65.1
17f + *E*-**9**	**a2-e**	*anti*	0	0	1.978	100.0	−166.5
	b1-e	*syn*	3.04	3.96	2.014	102.9	−63.8
	c1-e	*syn*	4.07	4.49	1.993	102.7	111.8
	c2-e	*anti*	4.12	4.84	2.008	108.2	23.6
17f + *Z*-**9**	**a2-e**	*anti*	0	0.05	1.978	99.9	−170.5
	b1-e	*syn*	0.77	0	2.026	102.9	−63.5
	a1-e	*syn*	5.17	4.17	1.985	98.3	−178.9
	b2-e	*anti*	5.86	3.26	1.976	106.6	−62.1
	c2-e	*anti*	6.29	5.89	2.017	108.4	23.5

[a] All geometrical parameters shown belong to the transition states located at $T = 195$ K.

of the two carbon atoms that form the new bond in the product. We found that the obtained one-dimensional potentials do not exhibit a maximum that could resemble a TS structure, but a shallow region where the first derivative is close to zero. This observation explains why no TS could be found, and why the energy oscillates during the optimization process without meeting the convergence criteria (default optimization convergence criteria as implemented in Gaussian 03). Replacing the SiH_3 group by $SiMe_3$ did not solve this problem; MPW1K could still successfully be applied only to the ketone-derived systems, while by employing B3LYP it was not even possible to identify all TSs for the aldehyde-derived systems anymore.

Thus, we scanned a number of other popular DFT functionals and found that only with the BH&HLYP functional it was possible to find all TSs in the gas phase for all simplified systems ($SiMe_3 \rightarrow SiH_3$) under investigation [for the systems involving **17c** and **17f**, the TSs **a1-z, a2-z, b1-z, b2-z, c1-z**, and **c2-z** with *Z*-configurated carboxenium ions were not searched for since prior semiempirical investigations (AM1) already predicted relative energies > 30 kJ mol^{-1}].

Obviously, the fraction of the nonlocal exact Hartree−Fock or Kohn−Sham exchange included plays a crucial role in the performance of the various functionals. The corresponding fraction in the MPW1K functional might be not large enough. The fact that BH&HLYP is robust and universal for all systems reported in this work confirms the positive evaluation of this method by Durant 10 years ago.[28b]

The selectivities calculated therefrom (Table 3, column a) already reproduce the synconvergent behavior for **16c** and the anticonvergent behavior for **16e**. However, synconvergent behavior was predicted for **16a** and **16b** as well, which is not in line with the experimentally determined selectivities. For the

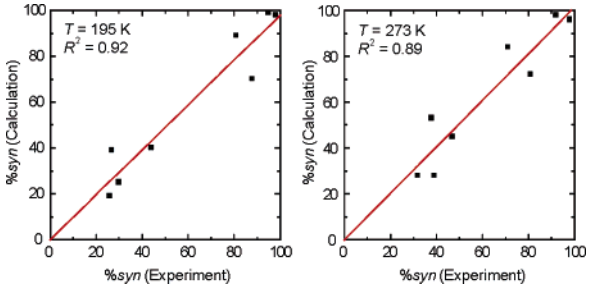

Figure 4. Calculated vs experimentally determined selectivities. The lines and R^2 values are derived from linear regression analysis. Experimental results are averaged experimental results from MCC and AS reactions, where applicable.

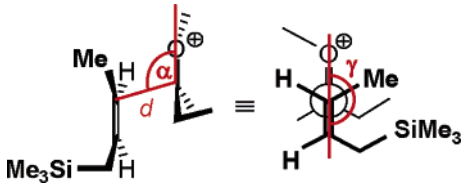

Figure 5. Selected geometrical parameters for the description of transition-state geometries using transition state **a2-e-b** for the system **17b** + *Z*-**9** as an example. *d* denotes the distance between the bond-forming carbon atoms (C···C), α is the angle of attack of the silane to the carboxenium ion double bond (Bürgi−Dunitz Angle, O═C···C), γ is the dihedral angle between the carboxenium ion and crotyl silane double bonds (O═C···C═C). Note that for the projection chosen above, γ has a positive (negative) value when the silane double bond is on the left-hand-side (right-hand-side). [Idealized transition-state conformation **a**: $\gamma = 180°$; **b**: $\gamma = -60°$; **c**: $\gamma = 60°$].

following investigations, we limited the TS conformations considered to those that are of relevance for the calculation of the selectivity (Figure 2).

We then decided to include the solvent dichloromethane, that was used for the experiments, in our calculations. At first, we calculated the free energy of solvation in *single point* calculations at the same level of theory as before, using the gas-phase geometries and adding the free energy correction term obtained from gas-phase frequency analysis. However, results were not satisfactory when employing either of the PCM, CPCM, or IPCM models[39] in combination with UAKS radii. Therefore, we performed optimizations and frequency calculations of the relevant TSs in dichloromethane solution using the PCM model and UAKS radii. We observed that it took typically about 5 to 10 optimization steps to meet the Gaussian 03 default convergence criteria when starting from the geometry obtained in gas-phase calculations, meaning that stationary points are different in gas phase and in condensed phase. Each calculation had to be performed once for $T = 195$ K and once for $T = 273$ K since the energy surface where stationary points are located in solution is temperature-dependent.

Obtained selectivities (Table 3, column b) are in closer agreement with experimental values, but still, synconvergent behavior was predicted for reactions involving **16a** and **16b**. In an attempt to model the real system as good as possible, we again replaced the SiH_3 group by the actual $SiMe_3$ residue and optimized the TSs for these actual systems in the solvent field. To be able to handle these systems computationally, the basis set had to be reduced from 6-31+G(d,p) to 6-31+G(d) by removing polarized functions at the hydrogen atoms. This reduction should not have any great influence on the accuracy

Chart 5. Relevant Transition States for **17e** + *E*-**9**; Hydrogen Atoms Are Omitted for Clarity, except for Aldehyde Protons and Double Bond Hydrogens

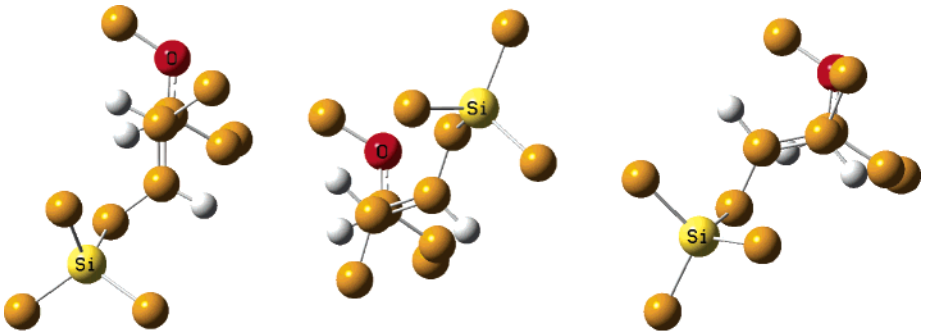

Chart 6. Relevant Transition States for **17b** + *Z*-**9**; Hydrogen Atoms Are Omitted for Clarity, except for Aldehyde Protons and Double Bond Hydrogens

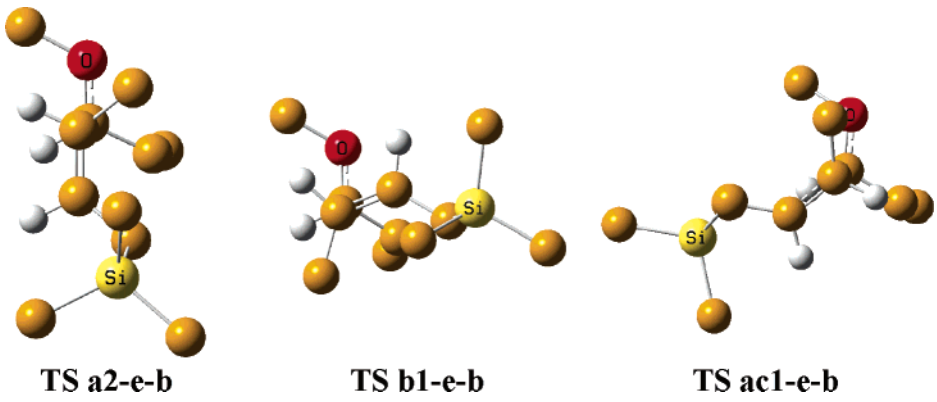

since there is no hydrogen atom transfer involved in the stereogenic step. Since BH&HLYP could not locate all necessary TSs, we again tested the MPW1K and B3LYP methods. It was not possible to find all TSs using MPW1K; however, B3LYP could now be successfully applied to almost all systems at hand (Table 3, column c).

Computationally predicted selectivities are in rather good agreement with experimental results (Figure 3). Furthermore, with exception of **17b** + *E*-**9**, the temperature dependence is very well reproduced. The exception is probably due to the very small TS energy differences for that particular system (see Table 4) which are not accurately enough reproduced by the chosen method. Figure 4 plots predicted against experimentally determined selectivities and shows the appropriateness of the computational method chosen.

From these results, we conclude that the investigated addition step is in fact the stereogenic step in MCC and AS reactions, which furthermore indirectly indicates the prior formation of the carboxenium ion for both reaction paths.

3.3. Transition States. In this subsection, we present the relevant TS structures that lead to the observed stereoselectivity. For each aldehyde-derived system, optimizations starting from the idealized conformations **a1** and **c1** (see Charts 3 and 4) converged to the same eclipsed TS that is halfway inbetween these starting geometries, therefore termed **ac1**.

Relative free energies $G_{rel}^{\ddagger}$ for $T = 195$ K and $T = 273$ K, and geometrical parameters of relevant TSs obtained by optimization in solution at $T = 195$ K are given in Table 4. Figure 5 illustrates the selected geometrical parameters to describe and compare TS geometries. The TS geometries obtained at $T = 273$ K differ only slightly for the parameters given (maximum deviations *d*: 0.0038 Å, α: 0.12°, γ: 0.86°). Values for additional geometrical parameters are given in the Supporting Information.

Inspection of Table 4 reveals that the stereochemical outcome for all aldehyde-derived systems can be explained by analysis of three TS conformations, viz. **a2-e** (to anti), **b1-e** (to syn) and **ac1-e** (to syn). For the ketone systems **17e** + *E*-**9** and **17e** + *Z*-**9**, TS **a2-z** (to syn) must be considered instead of the TS **ac1-e** that is not existent. For the systems **17b** and **17e**, only TSs with the ethyl group pointing backward (denoted by the descriptor **-b**, see Figure 1) are relevant for the determination of the diastereoselectivity. Charts5 and 6 display the TS structures **a2-e**−**b**, **b1-e**−**b** and **ac1-e**−**b** for the reactions involving **17b** + *E*-**9** and **17b** + *Z*-**9**, respectively. Figure 6 illustrates the relative TS energies for the TSs **a2-e**, **a2-z**, **b1-e** and **ac1-e** for all systems.

For the idealized staggered and eclipsed TS conformations, the dihedral angle γ would be 180° for TS **a2-e**, −60° for TS **b1-e** and 120° for TS **ac1-e**. The actually calculated values differ partly significantly from the idealized values what can mostly be rationalized by steric hindrance of the involved substituents. The major steric interactions (SIs) for TSs **a2-e**, **b1-e** and **ac1-e** for the attack of *E*-**9** or *Z*-**9** are shown in Chart 7. However, electronic or stereoelectronic effects, or TS-solvent interactions might also play a role. Relating TS geometries to relative TS energies $G_{rel}^{\ddagger}$ on the basis of SIs is possible for systems where $G_{rel}^{\ddagger}$ is large. For the system **17b** + *E*-**9**, $G_{rel}^{\ddagger}$ is very small, indicating that the responsible effects are rather subtle.

TS **a2-e**, leading to the anti configurated product, is the lowest-lying TS for all ketone-derived systems and for the addition of *Z*-**9** to **17a** and **17b**. For ketones, TS **a2-e** lies energetically lower than the competing TS **b1-e** since the number of major SIs is smaller. This fact does not change when replacing *E*-**9** by *Z*-**9**, leading to the observed anticonvergent behavior. For the aldehyde systems, SI 1 is diminished since $R^1 = H$ which corresponds to the smaller distance from R^1 to R^3 of ∼2.7 Å as opposed to ∼3.1 Å for the ketone systems. This effect is larger in the case of *Z*-**9**, which is illustrated by the positive value of γ as opposed to the negative values for all other cases. Still, the dihedral angle between the carboxenium ion and the silane double bond is almost equal to the idealized value of 180° for all systems investigated except for those where **17f** is employed. The deviation in that case is due to SI 3 between the crotyl silane methyl group and the very bulky ^{t}Bu group which is minimized by turning the crotyl silane counterclockwise by 10 to 15 degrees. The value of the Bürgi−Dunitz angle of attack α of about 100° is almost identical for all systems. Its deviation from the ideal angle[43] of 107° is due to steric interaction 3.

TS **b1-e** accounts for the predominant formation of syn product in the reactions **17a** + *E*-**9** and **17b** + *E*-**9**, and plays the main role in the formation of the syn configurated minor

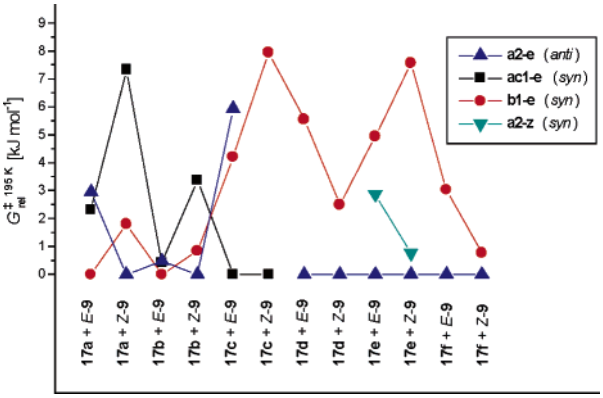

Figure 6. Relative transition-state energies $G_{rel}^{\ddagger}$, 195 K for the explanation of the stereoselectivity. The lowest-lying transition state for each system is arbitrarily set to 0 kJ mol^{-1}. For systems **17b** and **17e**, the transition states are **a2-e-b**, **b1-e-b**, **ac1-e-b** and **a2-z-b**. For systems involving **17d**, the transition states are **a2** and **b1**.

Chart 7. Major Steric Interactions (SIs) for Transition States **a2-e**, **b1-e** and **ac1-e**; $R^1 = H$ (for transition state **ac1-e**); H, Me (for transition states **a2-e** and **b1-e**); R^2 = Me, Et, ^{t}Bu; $R^3 = CH_2SiMe_3$

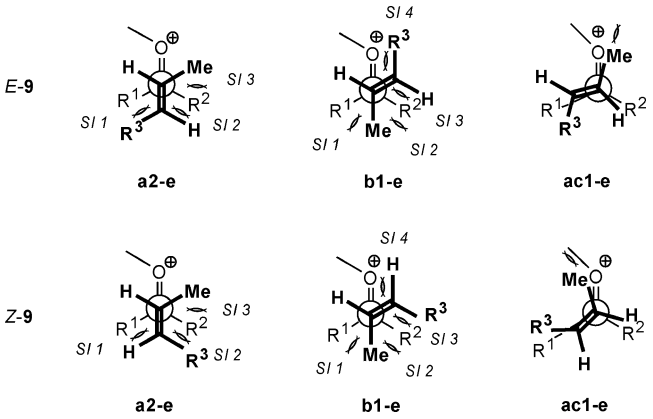

(43) Bürgi, H.; Dunitz, J. D.; Shepter, E. *J. Am. Chem. Soc.* **1973**, *95*, 5065−5067.

product in reactions **17a** + *Z*-**9**, **17b** + *Z*-**9**, and reactions involving **17f**. The deviation of γ from the idealized staggered model is about 5−10° for ketone-derived and about 10−15° for aldehyde-derived systems. In each case, the deviation is larger when *E*-**9** is employed which can be explained by the competition between SIs 1 and 3 with SIs 2 and 4. SI 1 is negligible for aldehyde-derived systems, leading to a larger absolute value of γ. Similar to TS **a2-e**, the distance of R^1 to the crotyl silane methyl group is about 0.3−0.4 Å smaller for the aldehyde-derived systems.

The comparison of the effects associated with TSs **a2-e** and **b1-e** allows for an explanation of stereoconservative behavior for systems **17a** and **17b**. TS **a2-e** is more stable for the attack of *Z*-**9** because SI 1 between two hydrogen atoms [*d* (H−H) = 2.60 Å for **17b** + *Z*-**9**] is less destabilizing than SI 1 between the aldehyde hydrogen atom and R^3 in the case of *E*-**9** [*d* ($\underline{C}H_2$-CH_3−H) = 2.90 Å for **17b** + *E*-**9**]. Additionally, TS **b1-e** is less stable for the attack of *Z*-**9** since, because of SI 3 [*d* ($\underline{C}H_2$-CH_3−$\underline{C}H_2SiMe_3$) = 3.38 Å for **17b** + *Z*-**9**], SI 2 cannot be minimized as for attack of *E*-**9** [*d* ($\underline{C}H_2CH_3$−$\underline{C}H_2SiMe_3$) = 2.95 Å for **17b** + *E*-**9**]. The combination of these effects leads to the observation that in case of *E*-**9** attack, syn selectivity is found (via TS **b1-e**), while the anti compound is formed when *Z*-**9** is employed (via TS **a2-e**).

Eclipsed TSs **ac1-e** that exist only for R^1 = H become more important as the aldehyde substituent R^2 size increases; this is the reason for the high selectivities for cases **17c** + *E*-**9** and **17c** + *Z*-**9**. The relative energy of TS **ac1-e** does not change when replacing *E*-**9** by *Z*-**9**, which can be explained by the fact that the only major SI is independent of the position of R^3. Once this only SI is lower than the combined SIs of any competing TS, (which is the case when R^2 is large), TS **ac1-e** is the lowest-lying TS. Resulting large TS energy differences lead to high syn selectivities regardless of substrate double bond geometry. The dihedral angle γ is about 105° (130°) for the attack of *E*-(*Z*)-**9**, which is probably due to subtle steric interactions between R^3 and the OMe-group or between R^3 and R^2. We conclude that a similar eclipsed TS is the reason for high syn selectivities observed in Lewis-acid catalyzed crotylations of larger aldehydes that eventually led to the classification by Denmark.[12]

TSs **a2-z** nicely illustrate the difficulties associated with **16e** as substrate with very similar substituents: Although TSs **a2-e** and **b1-e** exhibit an energy gap of 5−8 kJ mol^{-1} that would lead to a diastereoselectivity >96:3 at T = 195 K, TS **a2-z**, lying between, explains the observed lower anti diastereoselectivity. The geometrical features of TSs **a2-z** are almost identical to those of the corresponding TSs **a2-e** with the exception of the less stable carboxenium double bond geometry, which explains the rather small energy difference. Interatomic distances describing the SIs differ by less than 0.06 Å. For all other systems under investigation, TSs with *Z*-configurated carboxenium ions are not among the relevant TSs.

3.4. Activation Energies. Activation energies $\Delta G^{\ddagger}$ quoted in Table 5 for the stereogenic center forming step have been calculated as the energy difference between the sum of the substrate free energies and the lowest-lying TS for each system at T = 195 K and 273 K, and are obtained at the B3LYP/6-311+G(2d,p)/PCM/UAKS//B3LYP/6-31+G(d)/PCM/UAKS level of theory in dichloromethane solution. We note that the error of these values is much larger than for *differences* of $G^{\ddagger}$ values ($G_{rel}^{\ddagger}$) that are used to determine the stereoselectivities according to eq 1.

Table 5. Activation Energies $\Delta G^{\ddagger}$ for the Addition of *E*- and *Z*-Crotyl Trimethylsilane to *O*-Methyl Carboxenium Ions for T = 195 K and 273 K

entry	reaction	$\Delta G^{\ddagger}$, 195 K [kJ mol^{-1}]	$\Delta G^{\ddagger}$, 273 K [kJ mol^{-1}]
1	**17a** + *E*-**9**	24.0	37.5
2	**17a** + *Z*-**9**	21.3	34.5
3	**17b** + *E*-**9**	25.9	40.8
4	**17b** + *Z*-**9**	26.8	41.8
5	**17c** + *E*-**9**	52.7	66.9
6	**17c** + *Z*-**9**	51.8	66.9
7	**17d** + *E*-**9**	72.0	87.4
8	**17d** + *Z*-**9**	70.3	86.5
9	**17e** + *E*-**9**	82.7	97.9
10	**17e** + *Z*-**9**	78.6	93.8
11	**17f** + *E*-**9**	115.8	132.8
12	**17f** + *Z*-**9**	115.1	133.6

Scheme 6. Crotylation of Isobutyraldehyde

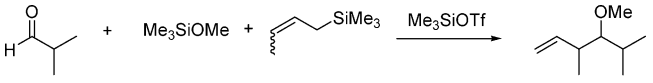

16g **18** **9** **19g**

The activation energy for the system **17a** + *E*-**9** could be determined in the same way as for the other systems because TS **b1-e** could be found for the actual system in dichloromethane solution employing the B3LYP/6-31+G(d) level of theory. The free energy of the carboxenium ion was calculated for its more stable *E*-configuration in all cases.

For the systems under investigation, aldehyde derived *O*-methyl carboxenium ions are generally more susceptible to nucleophilic attack than ketone-derived ions. For the systems involving **17f**, the very high activation energies would explain the low yields observed in experiment, although it is very likely that the formation of the mixed acetal and subsequent formation of the carboxenium ion involve elementary steps with even higher activation energies.

Activation energies do not differ greatly when replacing *E*-**9** by *Z*-**9**. Interestingly, $\Delta G^{\ddagger}$ strongly depends on temperature and rises by about 13−19 kJ mol^{-1} as temperature increases from 195 to 273 K.

4. Predictive Capability

By a comprehensive scan of a number of possible open TSs, we have found that three TSs are necessary and sufficient to calculate the syn/anti diastereoselectivity. Furthermore, we have shown that the B3LYP/6-31+G(d)/PCM/UAKS method is capable of determining TS energies for the MCC or AS reactions satisfactorily well.

This section is dedicated to examine whether the above statements hold when studying a new system. The MCC reaction of isobutyraldehyde (^{i}Pr-CHO, **16g**) with both *E*-**9** and *Z*-**9** at T = 273 K was chosen for investigation (Scheme 6). As one reviewer argued, these reactions are of great interest as **16g** mimics the synthetically mostly used monosubstituted α-chiral aldehydes.

Experiments were performed in the same fashion as described in section 3.1. Selectivities were determined via GC on achiral phase. TSs **a2-e**, **b1-e**, and **ac1-e** were found by employing the

Chart 8. Transition States for **17g** + *E*-**9**; Hydrogen Atoms Are Omitted for Clarity, except for Aldehyde Protons and Double Bond Hydrogens

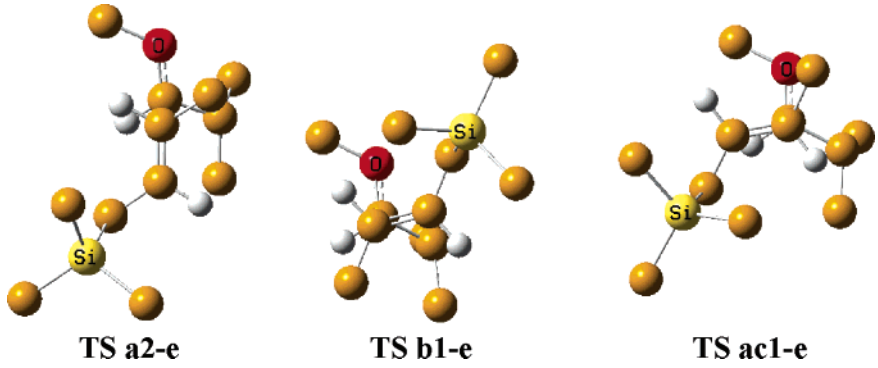

Chart 9. Transition States for **17g** + *Z*-**9**; Hydrogen Atoms Are Omitted for Clarity, except for Aldehyde Protons and Double Bond Hydrogens

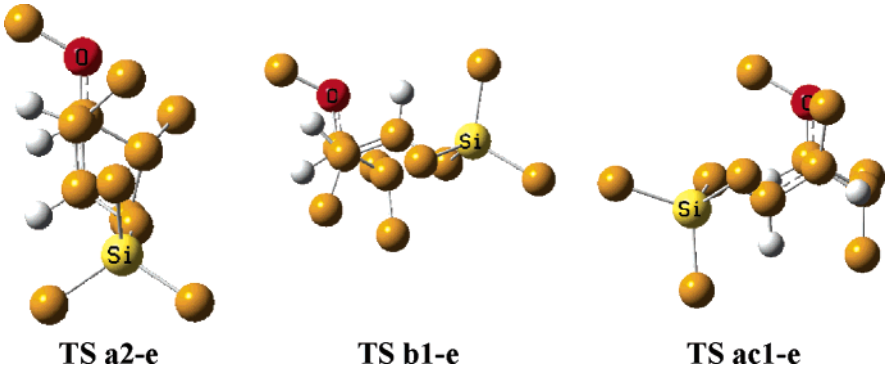

Table 6. Results for the MCC Reaction of Isobutyraldehyde (**16g**)

system	TS conformation	product stereochemistry	$G_{rel}^{\ddagger}$, 273 K [kJ mol^{-1}]	*syn*-**19g**:*anti*-**19g** calcd	*syn*-**19g**:*anti*-**19g** exptl
	a2-e	*anti*	2.68		
17g + *E*-**9**	**b1-e**	*syn*	1.47	**78**:22	**75**:25
	ac1-e	*syn*	0.00		
	a2-e	*anti*	2.49		
17g + *Z*-**9**	**b1-e**	*syn*	3.59	**83**:17	**85**:15
	ac1-e	*syn*	0.00		

B3LYP/6-31+G(d)/PCM/UAKS method at $T = 273$ K and are shown in Charts 8 and 9 for the attack of *E*-**9** and *Z*-**9**, respectively. Relative TS energies $G_{rel}^{\ddagger}$ and therefrom calculated predicted diastereoselectivities are given in Table 6, together with the experimental results.

Predicted and experimentally determined selectivities are in excellent agreement. We conclude that the selected TS conformations and the method chosen are sufficient to predict diastereoselectivities for MCC reactions.

5. Conclusion

We have studied the syn/anti diastereoselectivities of multicomponent crotylation (MCC) and acetal substitution (AS) reactions of simple aldehydes and ketones and have found that experimentally determined selectivities can be reproduced very well by computational investigations of the attack of *E*- or *Z*-crotyl trimethylsilane to *O*-methyl carboxenium ions. This and the fact that MCC and AS reactions are nearly identical in their stereochemical outcome let us conclude that these reactions indeed proceed via an S_N1-type mechanism. As there are only very small energy differences between the TSs, simplification of the systems can result in erroneously predicted selectivities. When performing computational investigations, optimizations and frequency calculations have to be performed with the actual system in the solvent field.

Crotylations of ketones lead to the anti product, while crotylations of larger aldehydes predominantly give the syn product. The double-bond geometry of crotyl trimethylsilane is irrelevant for the general stereochemical outcome in these cases. However, using smaller aldehydes such as acetaldehyde or propionaldehyde, stereoselectivity is reversed when replacing *E*- by *Z*-crotyl trimethylsilane. This stereochemical outcome can be rationalized by different steric interactions of open TSs. For the aldehyde-derived systems, an eclipsed TS, where the crotyl silane double bond lies "on top" of the aldehyde hydrogen atom, and the crotyl silane hydrogen lies "on top" of the larger aldehyde substituent, was found to be the lowest-energy TS when the aldehyde is large, leading to almost exclusive formation of syn product. Except for this TS, important TSs are those where the crotyl silane hydrogen is staggered between the smaller substituent of the carbonyl and the methyl group at the oxygen. Only when the substituents at the carbonyl group are very similar, the corresponding TS with exchanged substituents cannot be neglected.

Neglecting any but steric interaction between the Lewis acid and crotyl silane, we can predict that Lewis-acid-catalyzed crotylations of larger aldehydes should give the syn homoallylic alcohol, while the anti product should be formed when employing ketones. However, because the major steric interaction in the eclipsed TS depends on the size of the Lewis acid, it is

possible that the selectivity is lower or even reversed when crotylating aldehydes with larger Lewis acids. We can further extent the prediction of simple syn/anti diastereoselectivity to reactions with crotyl tributylstannanes as these have been classified to proceed via equivalent open TSs.

Acknowledgment. This work has been supported by the *Fonds der chemischen Industrie*. We thank the *Gesellschaft für wissenschaftliche Datenverarbeitung Göttingen (GWDG)* for providing access to their computing resources. T.K. thanks the *Studienstiftung des Deutschen Volkes* for a scholarship.

Supporting Information Available: Complete ref 36, experimental procedures, spectral data, tables of absolute energies, table of interatomic distances for relevant TSs, IRC plots, and Cartesian coordinates for all substrates and relevant transition states calculated at 195 K in solution. This material is available free of charge via the Internet at http://pubs.acs.org.

JA062528V